Oxygen diffusion and surface exchange coefficients determined under high pressure: comparisons between oxygen deficient vs. oxygen over-stoichiometric air electrode materials

Jérôme Laurencin, Aurelien Flura, Giuseppe Sdanghi, Sébastien Fourcade, Vaibhav Vibhu, Jean-Paul Salvetat, Jean-Marc. Bassat

B1503

Oxygen diffusion and surface exchange coefficients determined under high pressure: comparisons between oxygen deficient *vs.* oxygen over-stoichiometric air electrode materials

Jérôme Laurencin* (1), Aurélien Flura (2), Giuseppe Sdanghi (1,2), Sébastien Fourcade (2), Vaibhav Vibhu (3), Jean-Paul Salvetat (4) and Jean-Marc Bassat* (2)

(1) CEA Grenoble, DRT/LITEN/DTBH/SCSH, 38054 Grenoble, France

(2) CNRS, Univ. Bordeaux, Bordeaux INP, ICMCB, 33600 Pessac, France

(3) Institute of Energy / Climate Research, IEK-9, FZJ GmbH, 52425 Jülich, Germany

(4) CNRS, Placamat, UMS 3626, 33600 Pessac, France

Tel.: +33-6-51-87-43-12

* jerome.laurencin@cea.fr; *jean-marc.bassat@icmcb.cnrs.fr

Abstract

MIEC (Mixed Ionic Electronic Conductors) oxides combine, in addition to a high electronic conductivity, high oxygen diffusivity (D) and oxygen surface exchange (k) coefficients. These properties can be directly determined thanks to the so-called IEDP (Isotopic Exchange Depth Profiling) method, which leads to determine the tracer coefficients D* and k*. To date, the reported measurements in the literature have been performed at ambient pressure and even below. However, for a higher efficiency of hydrogen production at the system level, or for a 'Power-to-Gas' application, it is envisaged to operate the Solid Oxide Electrolysers (SOE) at high pressures, between 10 to 60 bars. In this frame, it becomes *mandatory* to assess the oxygen reduction/oxidation and the transport properties of the oxygen electrodes materials in the operating conditions, *i.e.* when there are submitted to such high pressure (HP) at high temperature.

In order to address these questions, an innovative setup able to operate up to a total pressure of 50 bars and 900°C has been developed in collaboration between ICMCB-CNRS and CEA-LITEN. The setup, which has been already described, has been used here to measure the properties of classical MIEC materials for SOE applications. Our main goal was to compare the behaviour of two different kinds of oxides considered as references: the La-Sr-Fe-Co perovskites, which are oxygen deficient, and nickelates with the K_2NiF_4-type structure, which include interstitial oxygen. Oxygen exchanges have been performed at 500 < T°C < 700 and under P (air) = 30 bars ($p(O_2) \sim 6.5$ bars).

In comparison to the atmospheric condition, the oxygen stoichiometry is significantly increased after the oxygen exchanges performed under pressure, in all cases, as expected. Experimental results (D* and k*) obtained on both kind of oxides will be presented, compared and discussed. More specifically, the evolution of the surface exchange with the pressure is confronted to theoretical predictions based on analytical considerations. The good agreement between the experimental data and the model results tends to prove the accuracy of the measure and it allows better explaining the dependency of the surface exchange coefficient with the oxygen partial pressure.

Introduction

Clean and sustainable energy sources are currently becoming essential. However, since the renewable energies are intermittent, efficient solutions for their storage are required, to match the fluctuations between the demand and the production. In this frame, hydrogen is considered as one of the most efficient energy vector [1]. High Temperature Steam Electrolysis (HTSE), based on the Solid Oxide Electrolysis Cells (SOEC) technology, is a promising and attractive technical solution for hydrogen production at high efficiency [2]. A technical issue is that hydrogen has to be stored and distributed at high pressure. Indeed, since the compression of liquid water consumes much less energy than gaseous hydrogen, it is advantageous to perform the steam electrolysis directly under pressure [3]. Moreover, the high-temperature co-electrolysis of steam and carbon dioxide enables to convert electricity into a syngas composed of carbon monoxide and hydrogen [2, 4]. This gas mixture can be transformed in a second step in liquid or gaseous hydrocarbons with conventional catalytic processes working at high pressure between 10 and 100 bars [5]. In this case, an integrated system working directly under pressure could also be beneficial in terms of efficiency and cost [3, 6]. In this context, it is mandatory to investigate the impact of high pressure on the electro-catalytic properties of the electrode materials that control the cell electrochemical response, and more particularly the oxygen electrode.

Mixed Ionic Electronic Conductors (MIEC) are commonly used as oxygen electrodes in SOEC cells. In addition to a high electronic conductivity, this type of electrode material require both high oxygen diffusivity and surface exchange coefficient (D and k, respectively) at the operating temperatures. Two different kind of efficient candidates are generally considered: i) the oxygen deficient perovskites such as $La_{0.58}Sr_{0.4}CoO_{3-\delta}$ (LSC) and $La_{0.58}Sr_{0.4}Fe_{0.8}Co_{0.2}O_{3-\delta}$ (LSFC) [7], which are nowadays the standard SOEC materials and ii) the oxygen over-stoichiometric oxides, such as nickelates $Ln_2NiO_{4+\delta}$ (Ln = La, Pr, Nd), which belong to the so-called Ruddlesden series $Ln_{n+1}Ni_nO_{3n+1}$ (here with n=1). These more innovative compounds with the K_2NiF_4 -type layered structure have shown promising oxygen electrode performances because of their large anionic bulk diffusion and surface exchange coefficients, combined with a good electrical conductivity and a thermal expansion coefficient matching with those of other cell components [8, 9].

To date, the reported measurements of D and k in the literature have been performed at ambient pressure and even below [10]. However, to the best of our knowledge there is no available data measured at high pressure whatever the considered electrode material.

1. Scientific Approach

The objectives of the current work consist in: 1) performing isotopic oxygen exchanges on dense pellets with $Ln_2NiO_{4+\delta}$ (Ln = La, Pr, Nd), LSC and LSFC compositions under high oxygen pressure, 2) checking that the resulting oxygen stoichiometry δ was significantly changed after such exchanges and 3) evaluating the consequence of δ variation on the tracer D* and k* coefficients.

2. Experiments/Calculations

Dense samples in pure materials with a density of at least 95% are required for the oxygen exchange experiments. In this study, pellets were prepared to fulfill these conditions, with a diameter of roughly 20 mm after sintering.
Pure powders of the three lanthanide nickelates were produced using the modified Pechini method [11] from Pr_6O_{11} (Aldrich chem, 99.9%), La_2O_3 and Nd_2O_3 (Strem Chemical, 99.99%) and $Ni(NO_3)_2{,}6H_2O$ (Acros Organics, 99%) precursors. La_2O_3 powder was initially heat-treated at 900 °C overnight to remove residual water before weighing. The final annealing was performed at 1200 °C for 12 h in air, leading to well crystallized phases. The purity of the powder was controlled by X-ray Diffraction (XRD) analysis. The materials were then sintered at 1350 °C for 4 h in order to get dense pellets. $La_{0.58}Sr_{0.4}Fe_{0.80}Co_{0.2}O_{3-\delta}$ (LSFC) and $La_{0.58}Sr_{0.4}CoO_{3-\delta}$ (LSC) powders were synthesized by a standard solid-state route using following precursors: La_2O_3 (99.99%, Sigma Aldrich), $SrCO_3$ (99.9%, Sigma Aldrich), Fe_2O_3 (99%, Sigma Aldrich) and Co_3O_4 (99%, Alfa Aeser). The powders were weighed according to the compositions and then ball-milled for 4 h at 250 rpm using zirconia balls and isopropanol (98.8%, VWR). After drying at 80 °C overnight, the mixtures were then calcined in air at 1080 °C for 8 h. After getting the pure phase, the powders were again ball-milled for 4 h in order to get the average particle size ~1µm. The dense pellets of LSFC and LSC were prepared by uniaxial pressing of the powders followed by a sintering at 1350 °C for 4 h.
For the five studied compositions, the dense pellets were first mirror polished, using abrasives of decreasing grain diameter, then diamond paste to complete the work. Finally, cubes of roughly 4 mm side length were cut from the pellet, using a diamond cutting-disc (Isomet Buehler), in order to ensure that our samples are comparable.

The isotopic oxygen exchange setup was developed for an operation under total pressure up to 40 bars (Fig.1) and temperature up to 1100°C. It was more extensively described in [12]. The first line of the setup is dedicated to pumping: using a turbomolecular pump a vacuum of roughly 10^{-6} mbar is obtained. The marked ^{18}O gas (with purity close to 98%) is routed through a second line, from a gas (air) cylinder provided by Euriso-top company with the following specifications: 1L, P = 20 bars. Another line is dedicated to ^{16}O from the laboratory. A fourth line is dedicated to cryo-pumping of the marked ^{18}O at the end of the exchange, which is achieved by immersing an stainless steel rod (one meter long) into liquid helium. The gas may then be used for another experiment, provided that the ratio $^{18}O/^{16}O$ is still high. Two manometers allows measuring respectively the low and high pressures.

Fig.1 – Original isotopic exchange setup for experiments up to P = 40 bars and T=1100°C

The sample holder is a closed cylinder made of magnesium doped zirconia: it was designed to withstand both the high pressure and high temperature in steady state operation and also the stresses induced by quick thermal quenching. It was thus able to withstand, through all our experiments, rapid cooling from high operating temperature (700°C - 500°C) down to room temperature. This thermal quenching was achieved by removing the sample holder from the sliding furnace mounted on rails.
In a first step, the samples were equilibrated at the target temperature (700 °C for instance) in $^{16}O_2$ for a period at least ten times longer than the one chosen for the oxygen exchange experiment, then quenched down to room temperature. This treatment creates the baseline in $^{18}O/^{16}O$ inside the sample that will be used as reference later during the TOF-SIMS analyses. Besides, it fixes the chemistry in the bulk of the materials: the oxygen over-stoichiometry of the lanthanide nickelate and the oxygen under-stoichiometry in the perovskites. Next, the $^{16}O_2$ gas was pumped and replaced with the desired pressure of $^{18}O_2$ at room temperature. The samples were quickly heated to reach the target temperature, and the oxygen exchange experiments carried out for a determined time. Typically, the duration times used for the oxygen exchange steps varies from about 90 min. at 700°C till about 20h at 500°C. Samples were finally quenched down to room temperature, and $^{18}O_2$ recovered using liquid helium. Finally, the samples were taken out of the zirconia cylinder to be prepared for the Time-of-Flight Secondary Ion Mass Spectrometry (TOF-SIMS) analyses.

Our first goal was to determine the delta (δ) value characterizing the oxygen under/over-stoichiometric of the oxides, after each thermal treatment performed under pressure followed by a thermal quenching. For this purpose, Thermogravimetric Analysis (TGA) experiments were carried out using a TA Instrument® TGA-5500 device. First, the dense bare samples (after exchange experiments) were crushed into powder using mortar-pestle. Then the powders were heated under air up to 150 °C/1h, then cooled down to room temperature with a slow rate (2 °C.min^{-1}), with the aim to remove any traces of water. A second cycle was performed under Ar - 5% H_2 flux with a very slow heating rate of (0.5 °C.min^{-1}) up to 1000 °C. The full decomposition of the material under reducing atmosphere leads to the determination of the oxygen stoichiometry after cycling the sample down to room temperature. The decomposition products (Ln_2O_3, SrO, metallic Ni, Fe and Co) were verified by XRD after the thermal cycle. However, despite several attempts, the complete reduction of LSFC under Ar - 5% H_2 flux was never reached (the XRD analyses evidenced the formation of $(La,Sr)_2(Fe,Co)O_4$ + Fe + Co) making the calculation of δ not possible in this case.

Prior to the TOF-SIMS analyses, the cubes were cut in half with the utmost care using the diamond cutting-disc. This cut is necessary to reveal the gradient in ^{18}O. The new face created was then mirror polished. The resulting two samples were pressed altogether and fixed inside a stainless-steel ring with Wood's metal alloy. The particularity of this preparation is that one of the samples exposes the surface of the cube that was in direct contact with $^{18}O_2$, while the other sample exposes the bulk of the cube that contains the gradient of ^{18}O. The benefit of this setup is to measure with precision the ratio $^{18}O/^{16}O$ at the surface of the sample, averaged over a large area. This value is used as the origin of the gradient measured on the other sample.

SIMS experiments were performed using a TOF SIMS 5 (IONTOF, Münster, Germany).

Samples were analysed in spectroscopy mode by scanning a primary 30 keV Bi^+ beam over 500x500 μm^2 area, interlaced with a 1 keV Cs^+ sputter beam scanned over 600x600 μm^2 to eliminate surface impurities and enhance production of negative secondary ions. Area of interest was adjusted using the integrated optical camera and sample stage controls so that a sample edge was located vertically on the right or left of the raster field of view. Data acquisition was started in the 3D mode, and the following procedure was used to determine the stopping condition: once the secondary ions of interest (e.g. ^{18}O and ^{16}O) peaks were selected on the spectra subpanel, images of ion intensity with definition 256 x 256 pixels were automatically generated by the instrument software (SurfaceLab 7) in the image stockpile subpanel. The images of ^{18}O and ^{16}O intensities are then combined to generate an image of the isotopic ratio of interest $I(^{18}O)/(I(^{18}O)+I(^{16}O))$, and performed an average line scan thereof, using the X-area feature of SurfaceLab linescan editor. Using this procedure we could follow the gradient line-scan progress in real-time so that data acquisition could be stopped, typically after 5 to 10 min, when the gradient was stabilized at a good S/N ratio. Doing so an isotopic ratio profile averaged over a volume of approx. 500X500X0.1 μm^3 is generated, which minimizes artifacts from impurities and inhomogeneities. The data were finally exported as ASCII file for further analysis. In some cases, ^{18}O gradient spanned over 500 µm so that a second adjacent area was analysed similarly and stitched to the previous one.
The experimental oxygen profiles (evolution of $I(^{18}O)/I(^{18}O)+I(^{16}O)$ *vs.* depth) were then fitted using the Crank solution to the equation of the second Fick's law of gas diffusion in solids [13, 14], which leads determining the D* and k* coefficients (* being relative to the diffusion of the ^{18}O tracer).

3. Results and discussion

After the oxygen exchange steps, the samples were quenched to stop the oxygen diffusion in order to keep the same oxygen composition that was reached in the material during the investigated experimental conditions. Our first goal was to determine the corresponding oxygen stoichiometry values and, for this purpose, we used TGAs experiments performed under reducing atmosphere ($Ar/5\%H_2$ flow) on powders (crushed pellets). Regarding nickelates with oxygen over-stoichiometry, the decomposition of the oxide occurs in two steps: 1) At intermediate temperature a first plateau is evidenced, which corresponds to the stabilization of the oxide only containing Ni^{+II}, *i.e.* a composition $Ln_2NiO_{4.0}$ (Ln=La, Pr, Nd). The measured weight loss between room temperature and this temperature corresponds exactly to the disappearance of the oxygen over-stoichiometry δ; 2) in a second step, at higher temperature the full decomposition of the oxide is observed, leading as checked by XRD to the formation of Ln_2O_3 *plus* metallic Ni. Measuring the weight loss recorded between room temperature and the full reduction is then a second way to determine δ. On the contrary, regarding LSC only the full reduction is observed on the TGA curves. Table 1 gathers the results obtained for each exchanged sample, for $500 < T°C < 700$ and $pO_2 = 6.5$ bars (total pressure around 30 bars). Again, no experimental data are available for LSFC. For the nickelates, each reported δ value is an average between the two calculations detailed above.

Table 1. Oxygen over / under - stoichiometry's δ values determined by TGAs experiments performed under reducing atmosphere, on the samples previously exchanged under ^{18}O atmosphere, at a given temperature, under pO_2 = 6.5 bars

Exchange T°C	$La_2NiO_{4+\delta}$	$Pr_2NiO_{4+\delta}$	$Nd_2NiO_{4+\delta}$	$La_{0.58}Sr_{0.4}CoO_{3-\delta}$	LSFC
500	δ= 0.25	δ = 0.31	δ = 0.29	δ = 0.01	-
550	-	δ = 0.33	δ = 0.27		-
600	δ = 0.21	δ = 0.43	δ = 0.27	δ = 0.01	-
650	-	δ = 0.36	δ = 0.28		-
700	δ = 0.23	δ = 0.5	δ = 0.28	δ = 0.003	-

As expected, whatever the temperature used for the oxygen exchange, all the nickelates exhibit a significant increase of the oxygen over-stoichiometry after the thermal treatment performed under high oxygen pressure, compared to the value obtained after the chemical synthesis. Indeed, the compositions determined at room temperature after the synthesis performed in air were: $La_2NiO_{4.16}$, $Pr_2NiO_{4.22}$ and $Nd_2NiO_{4.21}$ (i.e. δ = 0.16, 0.22 and 0.21, respectively). It can noted that here is a large agreement in the literature regarding these values (see, for instance, [15] and the joined references). On another side, the oxygen under-stoichiometry of $La_{0.58}Sr_{0.4}CoO_{3-\delta}$ is reduced compared to the composition determined after the synthesis in air. Indeed, it is equal to δ=0.02 after synthesis whereas the samples after the thermal treatment performed under pressure become almost oxygen stoichiometric (table 1). This experimental result was also expected.
Finally, at this stage, our conclusion is that the studied compositions are significantly over-oxidized after the thermal treatments performed under ^{18}O pressure.

The evolutions of the D* and k* coefficients are plotted as a function of temperature in Fig. 2, 3 and 4 for the over-oxidized nickelates, *i.e.* $La_2NiO_{4+\delta}$, $Pr_2NiO_{4+\delta}$ and $Nd_2NiO_{4+\delta}$, respectively.

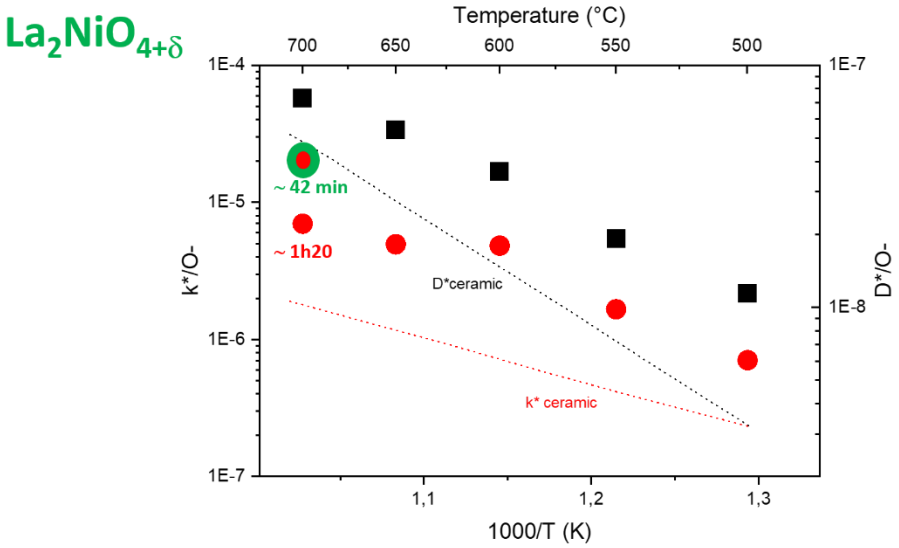

Fig.2 – Evolutions as a function of temperature of the k* (red dots) and D* (black dots) coefficients for over-oxidized $La_2NiO_{4+\delta}$ samples (table 1). The red and black dashed

lines give respectively the corresponding k* and D* data for isotopic exchanges performed under pO_2 = 0.2 bar (from [8])

The k* plot of $La_2NiO_{4+\delta}$ was quite peculiar, and we suspected that an experimental artifact for the measurements at 650°C and 700°C. Indeed, the exchange rate largely increases with increasing the temperature, in such a way that the surface of our sample can be saturated with ^{18}O if the exchange time is too long. In this case, the measured value of k* becomes inaccurate. To check this assumption, we reduced the exchange time at 700 °C from 80 min down to 42 min (red and green dot, respectively): we measured a k* value that is close to the linear regression plot of the k* values obtained at 500 °C, 550 °C and 600 °C.

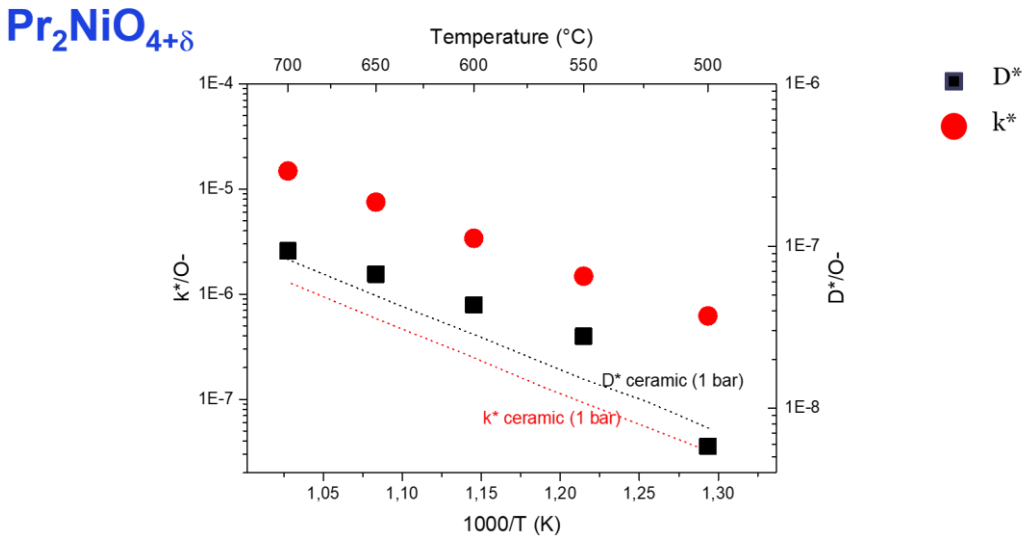

Fig.3 – Evolutions as a function of temperature of the k* (red dots) and D* (black dots) coefficients for over-oxidized $Pr_2NiO_{4+\delta}$ samples (table 1). The red and black dashed lines give respectively the corresponding k* and D* data for isotopic exchanges performed under pO_2 = 0.2 bar (from [8])

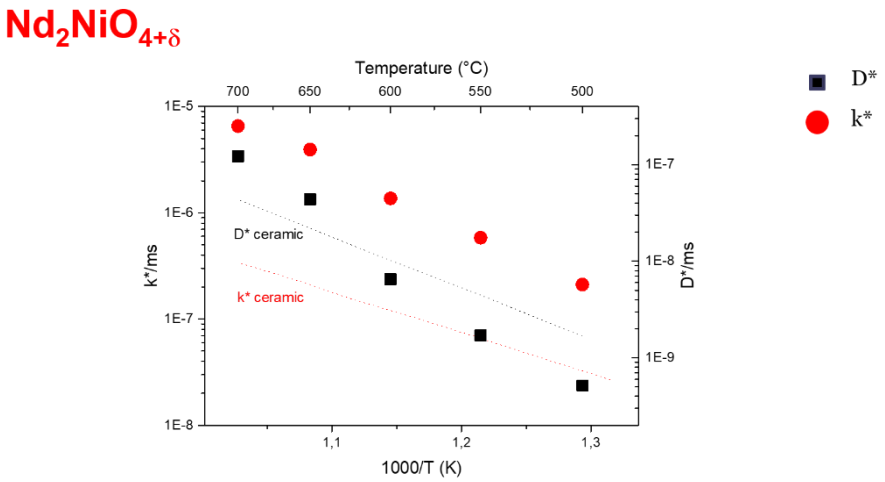

Fig.4 – Evolutions as a function of temperature of the k* (red dots) and D* (black dots) coefficients for over-oxidized $Nd_2NiO_{4+\delta}$ samples (table 1). The red and black dashed lines give respectively the corresponding k* and D* data for isotopic exchanges performed under pO_2 = 0.2 bar (from [8]).

Whatever the considered nickelate, both D* and k* coefficients are improved after oxygen exchanges performed under pressure compared to the corresponding values obtained after oxygen exchange performed under pO_2 = 0.2 atm. Considering the Nernst-Einstein relation, it can supposed that the ionic conductivity of such MIEC materials will be probably improved when operating under pressure (the measurements are in progress). It is of course a very interesting result leading to carefully consider these innovative oxygen electrodes for the SOEC application under pressure.

Some years ago Chroneos et al. [16], also Parfitt et al. [17] have performed Molecular Dynamics (MD) simulations regarding the oxygen diffusion in $La_2NiO_{4+\delta}$ and $Pr_2NiO_{4+\delta}$, respectively. The dominant mechanism of oxygen transport occurs *via* the network of apical oxygen sites connected by interstitial ion sites along a two-dimensional network (the so-called interstitialcy mechanism [16]). In the article by Parfitt et *al.*, the oxygen diffusivities were calculated for a range of hyper-stoichiometries, and an excellent agreement was found between the absolute calculated values and those observed experimentally. Initially (the first calculated point being δ = 0), the diffusivity rises very quickly as a function of δ, but rapidly levels off. Between δ = 0.05 and δ = 0.25 the diffusivity still increases but smoothly. The increase of the formation energy of oxygen interstitials, as well as a stiffening of the lattice cause by the additional oxygen interstitial pinning the NiO_6 sub-lattice, which reduces the passage of the oxygen ions, were involved. Our results are in good agreement with such calculations, indeed when increasing δ for each studied nickelate by means of oxygen pressure, we observed a limited increase of the diffusion coefficient, while a larger one could be expected in first approximation. The largest increase is observed when the initial oxygen over–stoichiometry is the lowest one, for $La_2NiO_{4+\delta}$ (δ = 0.16 at room temperature after annealing under air at normal pressure).

On the opposite, within this work, we also evidenced that the kinetic constant of oxygen exchange k* increases significantly with the pressure. This dependency is consistent with the theoretical evolution of the chemical kinetic constant k_{chem} (which is directly related to k*). Indeed, the reaction of oxygen insertion into the material can be written as follows:

$\frac{1}{2}O_2(gas) + \langle\ \ \rangle \leftrightarrow \langle O \rangle$	(1)

where $\langle O \rangle$ is the oxygen interstial and $\langle\ \ \rangle$ the empty site. The kinetic rate of this reaction is given by:

$v_1 = k_f (P_{O_2})^{1/2} y_{\langle\ \ \rangle} - k_b y_{\langle O \rangle}$	(2)

where k_f and k_b denote respectively the forward and backward kinetic constants of the reaction. The molar fraction $y_{\langle\ \ \rangle}$ and $y_{\langle O \rangle}$ are expressed through the concentrations in the material: $y_{\langle O \rangle} = \frac{C_{\langle O \rangle}}{C_{max}}$ and $y_{\langle\ \ \rangle} = \frac{C_{\langle\ \ \rangle}}{C_{max}}$ with $C_{\langle O \rangle} + C_{\langle\ \ \rangle} = C_{max}$. Assuming that the oxygen partial pressure in the gas phase is a constant imposed by the experimental conditions ($P_{O_2} = cte$), it can be easily shown that:

$v_1 = -\left[k_f (P_{O_2})^{1/2} - k_b\right]\left(y_{\langle 0 \rangle} - y_{\langle 0 \rangle}^{eq}\right)$	(3)

The kinetic rate of the oxygen exchange v_2 can be also expressed as $v_2 = -v_1 = k_{chem}\left(y_{\langle 0 \rangle} - y_{\langle 0 \rangle}^{eq}\right)$ [18]. The chemical constant is thus given by:

$k_{chem} = k_f (P_{O_2})^{1/2} - k_b$	(4)

Therefore, the chemical constant must increase with the square root of the oxygen partial pressure. This theoretical dependence is thus consistent with the experimental

increase of the kinetic constant k* with the pressure [18].

Fig. 5 and 6 plot the evolutions of the D* and k* coefficients *vs*. T, on the over-oxidized perovskites, *i.e.* $La_{0.58}Sr_{0.4}CoO_{3-\delta}$ (LSC) and $La_{0.58}Sr_{0.4}Fe_{0.8}Co_{0.2}O_{3-\delta}$ (LSFC), respectively.

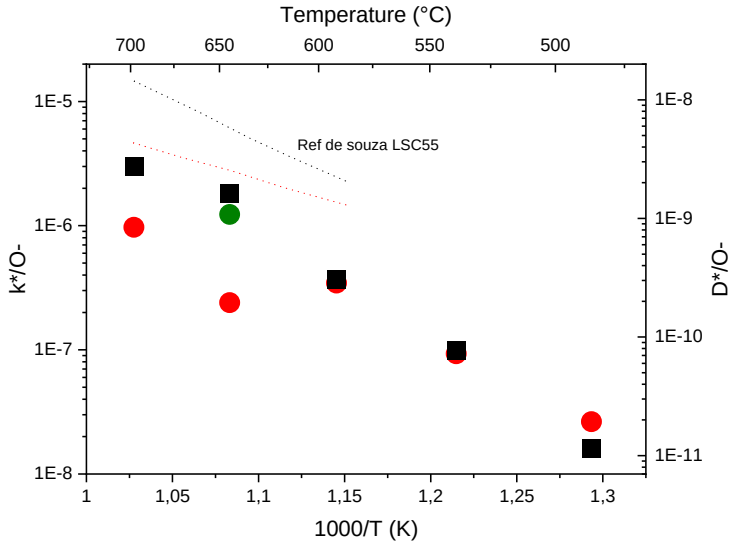

Fig.5 – Evolutions as a function of temperature of the k* (red dots) and D* (black dots) coefficients for $La_{0.58}Sr_{0.4}CoO_{3-\delta}$ (LSC, table 1). The red and black dashed lines give respectively the corresponding k* and D* data for isotopic exchanges performed under pO_2 = 0.2 bar (from [19]).

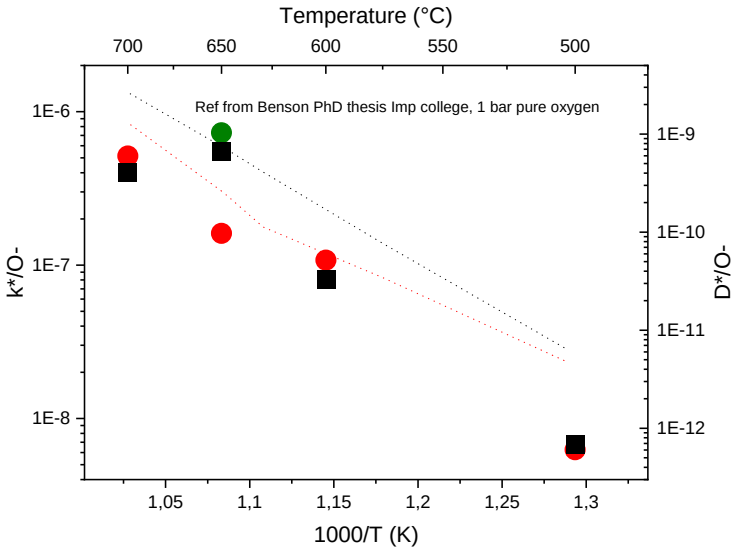

Fig.6 – Evolutions as a function of temperature of the k* (red dots) and D* (black dots) coefficients for $La_{0.58}Sr_{0.4}CoO_{3-\delta}$ (LSC, table 1). The red and black dashed lines give respectively the corresponding k* and D* data for isotopic exchanges performed under pO_2 = 0.2 bar (from [19]).

In both cases, at 650°C, we used two different exchange times (26h (red dot) and 2h (green dot)). Once again, as observed on $La_2NiO_{4+\delta}$, reducing the exchange time leads to an increase of the k* coefficient.
On the opposite to what was observed for the oxygen over-stoichiometric nickelates, D*

and k* coefficients for the oxygen deficient perovskites are found to decrease with increasing from pO_2 = 0.2 bar to pO_2 = 6.5 bar. This trend is especially pronounced for LSC, for which we have determined that the oxide became almost oxygen stoichiometric after the thermal treatment performed under pressure. Our hypothesis is that the oxygen vacancy concentration is too low to ensure the oxygen diffusion mechanism properly when the material is used under pressure. Regarding k*, the kinetic constant should increase as the square root of the oxygen partial pressure as predicted by eq. (4). For instance, this dependency was well retrieved by Katsuki et al. [18] for $La_{0.6}Sr_{0.4}Co_{0.8}Fe_{0.2}O_{3-\delta}$ over a range of low oxygen partial pressures changing from 10^{-4} atm to 1 atm at 800°C. This statement is also consistent with the results published by Elshof et al. [20]. Nevertheless, in our case, the kinetic constant for the investigated under-stoichiometric materials follows an opposite trend when increasing the oxygen partial pressure from 0.2 atm to 6.5 atm. This behavior remains still unclear. In ref. [18], the authors mentioned that 'further research seems necessary for a detail explanation of why k_{chem} decreases with reducing pO_2'. However, it seems that Eq. (4) could explain this evolution.

Conclusions

To increase the efficientcy at the system level, it is envisaged to operate the solid oxide electrolyser at high pressure. In this context, the goal of this work was to determine the oxygen diffusion and surface exchange coefficients (which characterize the O^{2-} ionic conductivity) of two standard under-stoichiometric oxygen electrode materials ($La_{0.58}Sr_{0.4}CoO_{3-\delta}$ (LSC) and $La_{0.58}Sr_{0.4}Fe_{0.8}Co_{0.2}O_{3-\delta}$ (LSFC)) compared to three over-stoichiometric nickelates ($La_2NiO_{4+\delta}$, $Pr_2NiO_{4+\delta}$ and $Nd_2NiO_{4+\delta}$). These latter materials have been developed for several years as alternative oxygen electrodes to the more conventional oxygen deficient perovskites. After a preliminary isotopic exchange step performed under high oxygen pressure, the measurements were performaed using the IEDP method was used. For this purpose, an original set-up has been developed.

As expected, the five materials became over oxidized after the oxygen isotopic exchanges performed in the temperature range 500 < T°C < 700 under $p(O_2) \sim 6.5$ bars compared to the as-prepared ones (under atmospheric condition at $p(O_2) \sim 0.2$ bars).

The measured evolutions of D* and k* coefficients are thus representative of materials in a very different oxidation state. It means first that the oxygen vacancy amounts of LSC and LSFC are largely reduced after the thermal treatments performed under pressure compared to that performed under pO_2 = 0.2 atm. Correspondingly, both the D* and k* coefficients values have been found significantly lowered when increasing the pressure up to 6.5 bar.

On the contrary, the oxygen over-stoichiometry of the nickelates is enlarged after the thermal treatment under pressure. Correspondingly, D* and k* coefficients of the oxygen over-stoichiometric nickelates are increased after oxygen exchanges performed under pressure. However, whatever the studied composition, the impact of pressure is less pronounced for D* compared to k*.

These statements would thus indicate that the electrochemical properties of such nickelates with MIEC properties are improved for a SOEC operation under pressure. They could thus constitute standard electrode materials for operations performed under oxygen pressure instead of Co-based perovskites. Indeed the interstitial amount of the nickelates structure can house a large range of oxygen corresponding to the over-oxidation of the electrodes, while on the contrary, the amount of oxygen vacancy in Co-

based perovskites becomes too low in the same operating conditions, limiting the ionic transport properties of the corresponding electrodes. Nevertheless, the long-term stability of these materials when submitted to high pressure and polarization still needs to be studied.

Acknowledgments

A.F. thanks the CNRS French grouping GDR HysPàc for supporting this research work *via* an internal project. CEA is acknowledged for its valuable technical aid, including the supply of the pressurized air bottle enriched in ^{18}O.

References

[1] - T.N. Veziroglu, F. Barbir, *Int. J. Hydrogen Energy* 17, 391 (1992).
[2] - S.D. Ebbesen, S.H. Jensen, A. Hauch and M.B. Mogensen, *Chem. Rev.* 114, 10697 (2014).
[3] - E. Giglio, A. Lanza,I, M. Santarelli, P. Leone, *J. Energy Storage* 1, 22 (2015).
[4] - Y. Wang, T. Liu, L; Lei, F. Chen, *Fuel Process Tech* 161, 248 (2017).
[5] - Catalysis in C1 Chemistry, Ed by W. Keim, D. Reidel Publishing company, 41 (1983).
[6] - J.B. Hansen, N. Christiansen, J.U. Nielsen, *ECS Transactions* 35(1), 2941 (2011).
[7] - M.Y. Lu, J.G. Railsback, H. Wang, Q. Liu, Y.A. Chart, S.-L. Zhang, S.A. Barnett, Journal of Materials Chemistry A, 7 (2019) 13531-13539.
[8] - E. Boehm, J.M. Bassat, P. Dordor, F. Mauvy, J.C. Grenier and P. Stevens; Solid State Ionics 176, 2717 (2005).
[9] - A. Aguadero, J.A. Alonso, M.J. Martinez-Lope, M.T. Fernandez-Diaz, M.J. Escudero and L. Daza, J. Mater. Chem. 16 (33), 3402 (2006).
[10] - J.A. Kilner, S.J. Skinner, H.H. Brongersma, Journal of Solid State Electrochemistry 2011, 15, 861.
[11] - P. Courty, H. Ajot, C. Marcilly, B. Delmon, Powder Technology, 7 (1) (1973) 21–38.
[12] - A. Flura, J. Laurencin, S. Fourcade, F. Mauvy, V. Vibhu, J.P. Salvetat, J. Mougin and J.M. Bassat, ECS Transactions 103 (1), 1319-1330 (2021).
[13] - J. Crank, “The mathematics of Diffusion”, 2nd ed.; Clarendon Press, Oxford, U.K., 1975.
[14] - J.M. Bassat, M. Petitjean, J. Fouletier, C. Lalanne, G. Caboche, F. Mauvy and J.C. Grenier, Applied Catalysis A: General 289, 84 (2005).
[15] - A. Flura, S. Dru, C. Nicollet, V. Vibhu, S. Fourcade, E. Lebraud, A. Rougier, J.M. Bassat, J.C. Grenier, *Journal of Solid State Chemistry* 228, 189 (2015).
[16] - A. Chroneos, D. Parfitt, J.A. Kilner and R.W. Grimes, *J. Mater. Chem*, 20, 2666 (2010).
[17] - D. Parfitt, A. Chroneos, J.A. Kilner and R. Grimes, *Phys. Chem. Chem. Phys.* 12, 6834 (2010).
[18] - M. Katsuki, S. Wang, M. Dokiya, T. Hashimoto, Solid State Ionics, **156**, 453 (2003).
[19] - S. Benson, PhD, Department of Materials, Imperial College London, 1999.
[20] - J.E. ten Elshof, M.H.R. Lankhorst, H.J.M. Bouwmeester, Solid State Ionics 99 (1997) 15– 22.